Steel and Composite Structures, *Vol. 23, No. 2 (2017) 187-194*
DOI: https://doi.org/10.12989/scs.2017.23.2.187

Load carrying capacity of CFRP retrofitted broken concrete arch

Peng Wang [1,3], Meirong Jiang [*1], Hailong Chen [1a],
Fengnian Jin [1b], Jiannan Zhou [1], Qing Zheng [3] and Hualin Fan [2,3c]

[1] *State Key Laboratory of Disaster Prevention & Mitigation of Explosion & Impact, PLA University of Science and Technology, Nanjing, China*
[2] *Research Center of Lightweight Structures and Intelligent Manufacturing, State Key Laboratory of Mechanics and Control of Mechanical Structures, Nanjing University of Aeronautics and Astronautics, Nanjing, China*
[3] *State Key Laboratory of Constructional Machinery, Zoomlion Heavy Industry Science & Technology Co., Ltd., Changsha, China*

(*Received July 10, 2016, Revised December 17, 2016, Accepted January 17, 2017*)

Abstract. To reuse a broken plain concrete (PC) arch, a retrofitting method was proposed to ensure excellent structural performances, in which carbon fiber reinforced polymers (CFRPs) were applied to repair and strengthen the damaged PC arch through bonding and wrapping techniques. Experiments were carried out to reveal the deformation and the load carrying capacity of the retrofitted composite arch. Based on the experiments, repairing and strengthening effects of the CFRP retrofitted broken arch were revealed. Simplified analysing model was suggested to predict the peak load of the CFRP retrofitted broken arch. According to the research, it is confirmed that absolutely broken PC arch can be completely repaired and reinforced, and even behaves more excellent than the intact PC arch when bonded together and strengthened with CFRP sheets. Using CFRP bonding/wrapping technique a novel efficient composite PC arch structure can be constructed, the comparison between rebar reinforced concrete (RC) arch and composite PC arch reveals that CFRP reinforcements can replace the function of steel bars in concrete arch.

Keywords: composite structures; failure/failure mode; fiber reinforced polymers (FRP); structural analysis

1. Introduction

Advanced fiber reinforced polymers (FRPs) have been widely applied in civil engineering to retrofit civil structures (Su *et al*. 2016, Bansal *et al*. 2016, Lu *et al*. 2015, and Chen *et al*. 2015). FRP strengthening method has also been applied to arch structures. Researchers have studied on the strengthening effects of FRPs in strengthening arch structures (D'Ambrisi *et al*. 2015, Chen 2002). It has been proved that FRP strengthening method is effective to improve the load carrying capacity of masonry arches and repair old and cracked arches.

Research group from Chongqing Jiaotong University has applied FRPs to strengthen RC arches through three strengthening schemes: (a) O-style; (b) U-style and (c) I-style reinforcements (Wang 2013, Sun 2013). According to the results, O-style strengthening method with enclosed FRPs is the most efficient method for the RC arch structure. Hamed *et al*. (2014) reinforced RC arches with externally bonded composite materials. The results reveal that applying the FRP strips leads to an increase of about 40% in the peak load of the arch, changes to the cracking pattern, and a significant increase in deflection capacity.

Researchers from State Key Laboratory of Disaster Prevention & Mitigation of Explosion & Impact of China have systematically discussed the strengthening efficiency of CFRP for underground RC arches under blast loads (Xie *et al*. 2014, Zhang *et al*. 2015, Chen *et al*. 2014, 2015). Results reveal that externally bonded CFRP sheets could restrict the development of the concrete tensile cracks and the CFRP strengthening arch fails at dynamic debonding induced by the reflective tensile wave. Then bonding/anchoring scheme was applied to rehabilitate the cracked arch, this method restrict the dynamic debonding of CFRP and let the composite arch have comparable load carrying capacity with the initial intact buried arch. They also applied CFRPs to strengthen statically-loaded RC arches, but the reinforcing effect of the bonding scheme is limited for semicircular arches. Dagher *et al*. (2012) proposed a novel concrete-filled tubular FRP arches for bridge structures, the composite arch structure without steel reinforcement exhibits excellent performances when applied in the construction of bridge or protective structures.

In our previous studies on CFRP reinforced PC arches, nine semi-circular PC arches were made and eight of these were reinforced by CFRPs. The internal radius of the arch is 500 mm (see Fig. 1). It's found that adopting discontinuously wrapping scheme (see Fig. 2(a)), load carrying capacity of the CFRP sheets reinforced arch achieves the level of RC arch and the composite arch has quasi-ductile deformation mode induced by a plastic mechanism. Adopting continuously wrapping scheme (see Fig. 2(b)), load carrying capacity of the CFRP reinforced arch is two times as that of RC arch and the composite arch fails at a brittle shear failure mode.

*Corresponding author, Ph.D. Student,
E-mail: jiangmeirong125@163.com
[a] Ph.D., E-mail: lona1185@126.com
[b] Professor, E-mail: jinfn2009@163.com
[c] Professor, E-mail: fhl02@mails.tsinghua.edu.cn

ISSN: 1229-9367 (Print), 1598-6233 (Online)

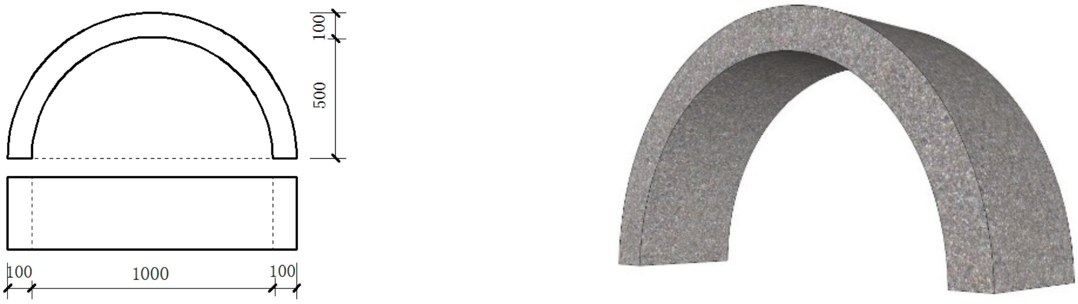

(a) Geometric dimensions (mm)

(b) Three-dimensional view

Fig. 1 Geometric characteristics of the PC arches

(a) Discontinuous wrapping scheme

(b) Continuous wrapping scheme

Fig. 2 CFRP reinforcing schemes of PC arches

Table 1 The definition of variables and constants

Variables	Definition	Constants	Definition	Value
P	Concentrated load	b	Thickness of arch	100 mm
N	Axial force of arch	h	Width of arch	300 mm
V	Shear force of arch	r	Radius of the semi-circular arch	550 mm
M	Bending moment of arch	A	Area of the arch cross-section	0.03 m^2
η	Utilizing efficiency of CFRP	λ	Maximum shear span ratio	3
X_1	Horizontal thrust	I	Second moment of cross-section	2.5×10^{-5} m^4
α	Central angle	σ_{ct}	Tensile strength of concrete	2.5 MPa
P_u	Peak load	σ_{cu}	Compressive strength of concrete	29 MPa
M_u	Maximum bending moment	σ_{fu}	Tensile strength of CFRP	3.4 GPa
V_u	Maximum shear resistance	α_1	Coefficient 1	0.0444
P_{fv}	Hooped strengthen ratio	α_2	Coefficient 2	1.25

Among these PC arches, one arch was broken into two segments in transport. In this paper, bonding/continuous-wrapping scheme was applied to repair and reinforce this completely broken PC arch. The novel and convenient repairing method is presented and the reinforcing effects were revealed and discussed through experimental researches. This retrofitting method can also serve as a good reference for repairing and strengthening masonry arches. Table 1 shows the variables and constants used in this paper.

2. Retrofitting method

To determine the potential of reusing the broken PC arch (see Fig. 3(a)), it was retrofitted with bonding/continuous-wrapping method. The repairing process consists of three operations. Firstly, the divided two segments were bonded together using epoxy resins (see Fig. 3(b)). Secondly, the joint was externally bonded together with short CFRP sheets (see Fig. 3(c)). Thirdly, long CFRP sheets were continuously bonded onto the intrados and the extrados of the new arch structure (see Fig. 3(d)). In order to fully utilize the excellent tensile-resist property of circumferential CFRP sheets, they were then entirely wrapped by hooped CFRP sheets, as shown in Figs. 2(b) or 4(a).

The circumferential CFRP sheets supply excellent bending resistance, especially anti-stretching ability of the concrete arch structure. While the hooped CFRP sheets

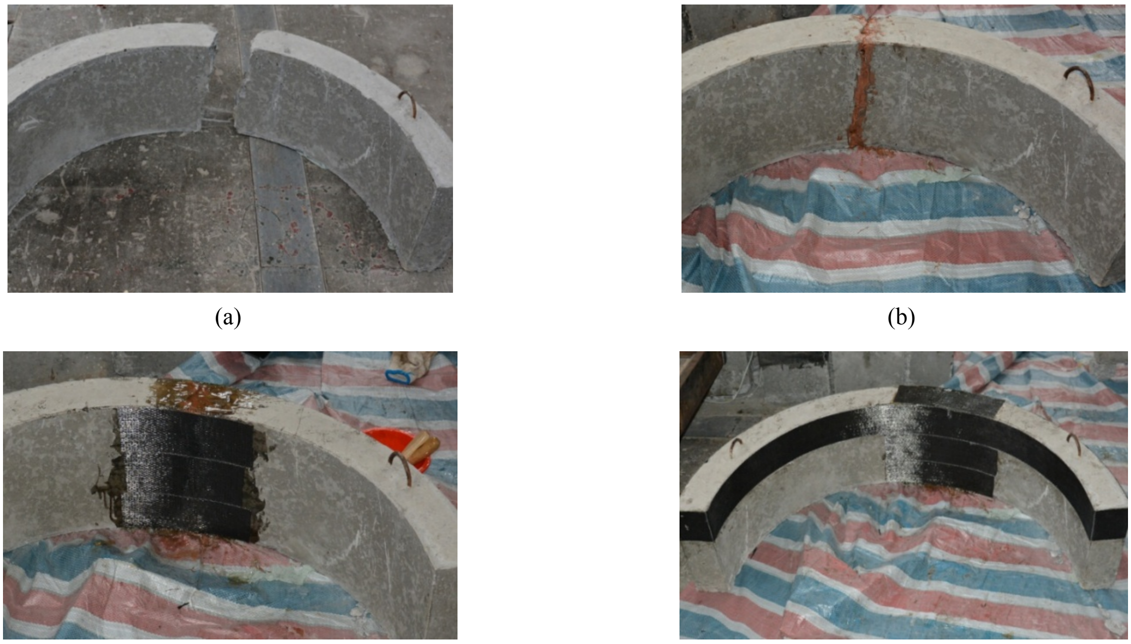

(a) (b) (c) (d)

Fig. 3 Repairing scheme of the broken arch

Table 2 Features of the CFRP reinforced PC arches

Arch	Extrados/strengthen ratio	Intrados/strengthen ratio	Lateral sides/strengthen ratio	Hoop/strengthen ratio
Retrofitted PC	CFRP sheet/0.167%	CFRP sheet/0.167%	CFRP sheet/0.11%	Continuous /0.11%
Strengthened PC	CFRP sheet/0.167%	CFRP sheet/0.167%	CFRP sheet/0.11%	Continuous /0.11%

restrict the debonding of circumferential CFRP sheets, increasing anti-shearing ability of the concrete cross section. The CFRP sheet is entirely made from carbon fiber cloth and epoxy resin, and the carbon fiber cloth used in experiments is unidirectional woven fabric with thickness of 0.167 mm and width of 100 mm. Its tensile strength and modulus under standard test are 3.4 GPa and 241 GPa, respectively. Using CFRP sheets to strengthen concrete arch is costly, but in this way the concrete cover and steel bars are saved and the construction method is not expensive.

Among these previous eight intact semi-circular PC arches, one PC arch has identical strengthening method with the broken PC arch. The strengthening features of the retrofitted PC arch and strengthened PC arch are shown in Table 2. The strengthen ratio is defined as the area of the strengthen material (carbon fiber cloth) used in per unit area of strengthened cross-section. The intrados and extrados of the two arches are both strengthened by CFRP sheets, and the strengthen ratio is $(0.167b)/(hb) = 0.167\%$. The lateral surfaces of the two arches are also bonded with CFRP sheets, the strengthen ratio is $(2\times0.167b)/(hb) = 0.11\%$. The bonded sheets are completely wrapped by sixteen hooped CFRP sheets. The continuous hoop reinforcement ratio is $(2\times0.167\times1000)/(1000h) = 0.11\%$. They are all sandwich arches.

3. Experimental researches

3.1 Method

Compression experiment was performed on the CFRP retrofitted PC arch structure and CFRP strengthened PC arch in order to check the repairing and strengthening effects, and another control PC arch without CFRP reinforcement is also tested for comparison. The arches were approximately pin-pointedly placed on a rigid steel frame and compressed by MTS 311.4 system whose maximum load capacity is 2500 Kn (see Fig. 4(a)). The lateral displacement of the arch was restricted by the side walls of a steel frame. So the constraint at the arch feet can be simplified as a pin-joint one. The load platen was placed on the extrados surface at the vault. The loading rate was controlled by the platen displacement at 1 mm/min when the vertical displacement was smaller than 10 mm and 3 mm/min when the displacement was beyond 10 mm. The arches were monotonically compressed to collapse.

Each arch was adhered with six strain gauges (see Fig. 4(b)), strains were measured twice per minute. Local deformations complicated the strain measurement. Though there were errors in the strain test, they could still supply valuable information for failure analysis of the arches.

3.2 Experimental results

The maximum load carrying capacity (peak load) of the PC arch without CFRP reinforcement is only 20.6 kN and the corresponding mid-span deflection is 5.26 mm, as

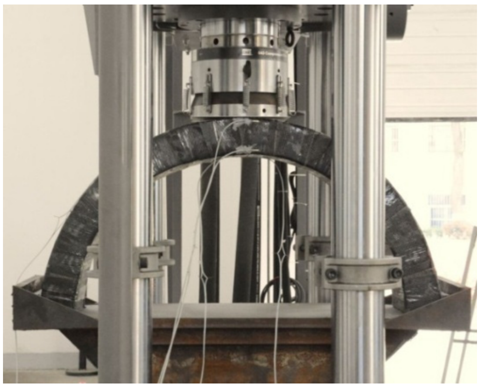

(a) MTS system

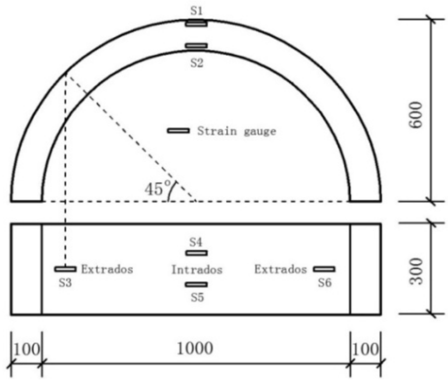

(b) Distribution of strain gauges(mm)

Fig. 4 Experimental protocol

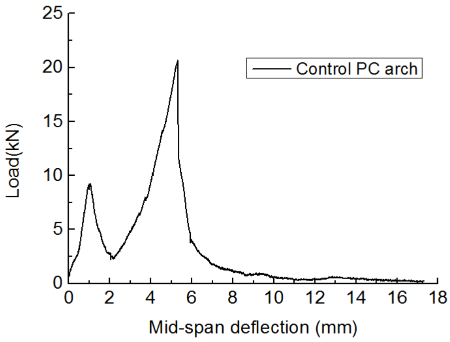

(a) Load-deflection curve

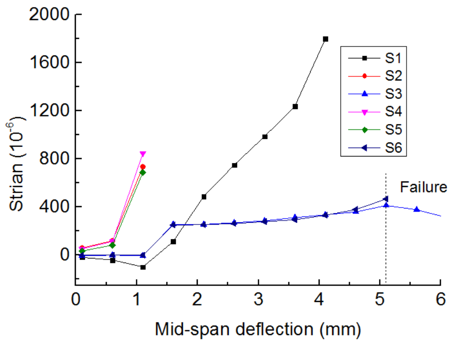

(b) Strain curves

(c) Collapse process

Fig. 5 Experimental results of the control PC arch

shown in Fig. 5(a). There have two zigzags in the load-deflection curve. At the first peak, strain on the intrados at the vault is about 800×10^{-6} (Fig. 5(b)), and strain gauges S2, S4 and S5 were broken off. The first zigzag of the load-deflection curve is caused by the concrete cracking on the intrados at the vault (Fig. 5(c)). For the convenience of analysis, the vertex of first zigzag is also defined as debonding point. When the concrete crack on extrados surface at the shoulders fully developed, the arch reached its peak load, and strains on the extrados at the shoulder are about 400×10^{-6} (Fig. 5(b)), measured by S3 and S6. Then a four-hinge collapse mechanism formed and the arch was completely destroyed and broken into three segments (Fig. 5(c)), the two broken joints located in the vault and near one shoulder of the arch, respectively. Strain gauge S1 (Fig. 4(b)) is located on the lateral side and close to the top surface of the vault. Strain in this position was negative initially and then turned to positive. Strain gauge S1 finally

Table 3 Experimental results of the concrete arches

Arch	Debonding load (kN)	Debonding deflection (mm)	Peak load (kN)	Failure deflection (mm)	Rigidity before debonding failure (kN/mm)
RC (Zhang *et al.* 2015)	45.2	4.56	106.1	22.24	9.91/6.62
PC	9.20	1.05	20.6	5.26	6.53/6.80
Strengthened PC	50.1	3.06	208.3	28.03	16.37/9.7
Retrofitted PC	44.3	3.75	170.3	22.71	11.81/13.51

Table 4 Measured strains of the concrete arches

Strains ($\times10^{-6}$)	PC arch		Strengthened PC arch		Retrofitted PC arch	
	Debonding	Failure	Debonding	Failure	Debonding	Failure
S1	-98		-427		-386	
S2	736		1401	6920	2080	
S3	-4	414	-60	4092	88	7530
S4	848		691	179	646	-1021
S5	688		628	-886	576	-207
S6	0	468	33	4494	0	932

failed under extension when the crack extended to the top surface of the vault.

The intrados and extrados of the strengthened PC arch are both reinforced by CFRP sheets, and the bonded circumferential sheets are completely wrapped by hooped CFRP sheets. The peak load reached 208.3 kN when the mid-span deflection is 21.9 mm (Fig. 6(a)).When loaded to 50.1 kN, the CFRP sheets delaminated from concrete surface at the vault (Fig. 6(c)), with the mid-span deflection of 3.06 mm, as listed in Table 3. Strain measured by gauge S5 is 628×10^{-6} at that time (Fig. 6(b)), as listed in Table 4. In consideration of the fact that the debonding strain of strengthened PC arch is not greater than that of control PC

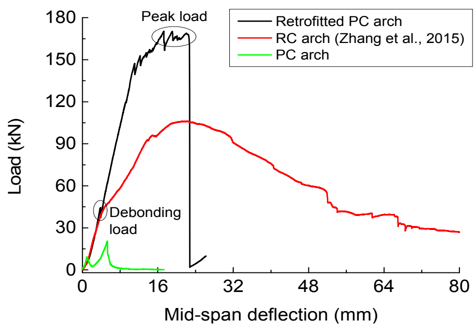

(a) Load-deflection curve

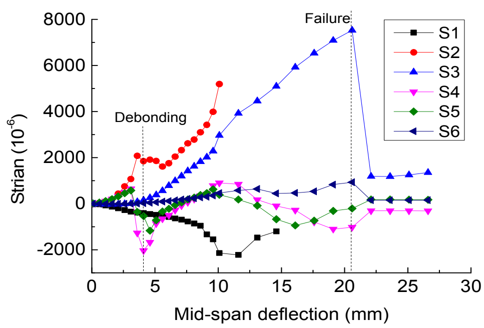

(b) Strain curves

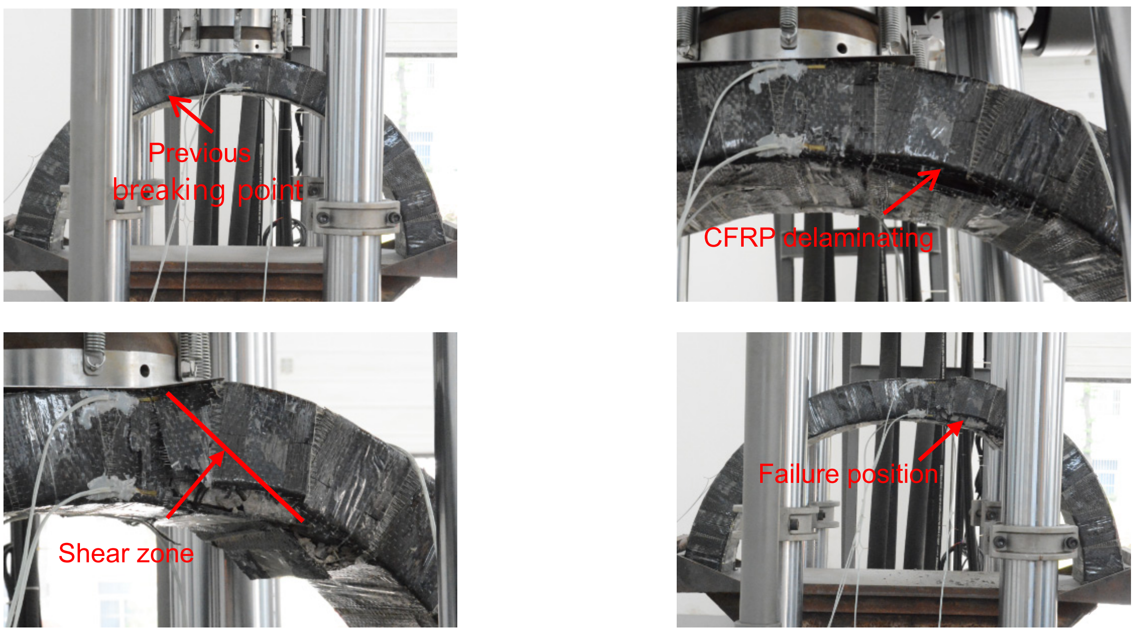

(c) Collapse process

Fig. 7 Experimental results of CFRP retrofitted PC arch

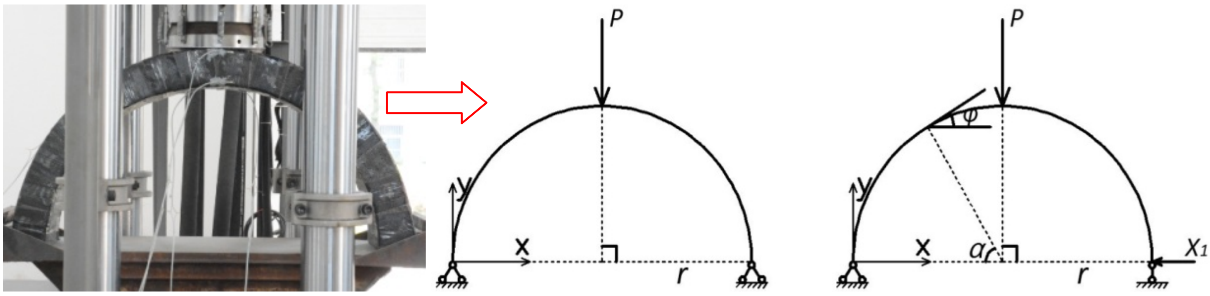

(a) Structural model

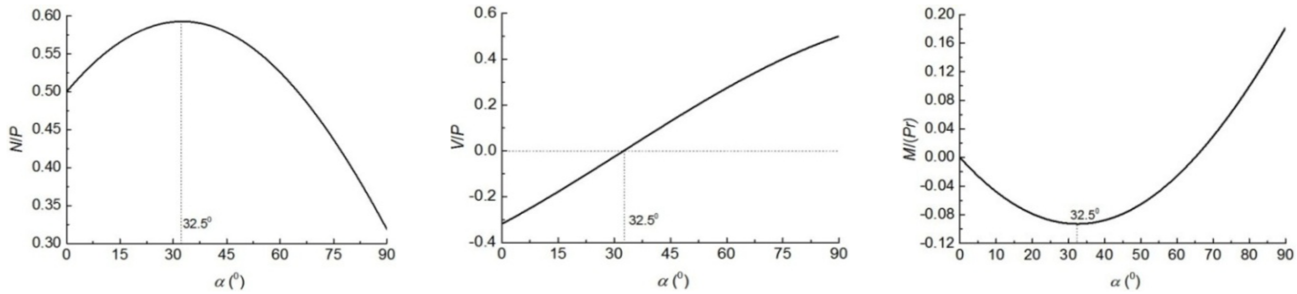

Axial force N Shear force V Bending moment M

(b) Distribution of the internal force

Fig. 8 Structural model of the indeterminate arch and the inner force

arch, the bending rigidity of the strengthened PC arch is enhanced by CFRP sheets. The tensile crack formed near the vault when the debonding load was achieved, but this extensional crack does not lead to ultimate failure of arch structure. The concrete is completely wrapped, and the CFRP system could keep the bending-resistance until the hooped CFRP sheets at the vault were pulled off by shear force at the mid-span. At that time, the mid-span deflection was extended to 28.03 mm. Shear failure at the vault induces a completely brittle failure mode for the strengthened composite PC arch.

The load-deflection curves of the control PC arch and the retrofitted PC arch are compared (see Fig. 7(a)). For better comparison, the curve of a RC arch (Zhang *et al.* 2015) is also plotted. The peak load of the arch retrofitted by CFRP is 170.3 kN, which is slightly smaller than that of the strengthened PC arch, but much greater than that of the PC arch. The arch failed by shearing near the vault (Fig. 7(c)), it's similar to the strengthened PC arch. But the shear failure of the retrofitted PC arch did not happened in the original broken position, so the retrofitting effect can be considered to be excellent. When the exerted load was going to 44.3 kN, the CFRP sheets delaminated from the concrete surface at the vault, the corresponding mid-span deflection was 3.75 mm, as listed in Table 3. Breaking of the hooped CFRP sheets and cracking of the concrete at the vault developed when the mid-span deflection was extended to 22.7 mm, which inducing brittle shear failure of the arch.

The debonding load and peak load of the retrofitted PC arch are far greater than that of the PC arch. The peak load of the retrofitted PC arch is 60.5% higher than that of the RC arch. In terms of the rigidities before debonding and before failure, the retrofitted PC arch is about twice larger than that of the PC arch, and slightly larger than that of the RC arch. It is interesting to find that the debonding loads and failure deflections of the retrofitted PC arch and the RC arch were very close to each other, this phenomenon may be related to the strength of concrete.

For each experimental condition, there is only one corresponding arch been loaded to failure, so there may be some uncertainties in the reliability of the experimental results, but the current research is helpful to follow-up study of composite arch structures.

4. Analyses

Destruction of the control PC arch is determined by the tensile cracking of the concrete at the vault and the shoulders. Without any reinforcement, the strength of the PC arch is only 20.6 kN. The experimental results indicate that the CFRP sheets play an important role in improving load carrying capacity of the CFRP reinforced arch. To fully utilize its excellent extensional property of CFRP, the CFRP reinforcements must be tightly wrapped by hooped CFRP sheets to restrict delaminating and to ensure that it is deformed compatibly with the concrete arch.

To get a better understanding of CFRP strengthening mechanism of composite arch structure, a simplified theoretical model is presented in this section to estimate the load carrying capacity of static loaded composite arches.

As shown in Fig. 8(a), the arch is approximately simply supported and loaded by a concentrated load, P, at the vault. The internal forces of arch structure are expressed as

$$\begin{cases} N = F_S^0 \sin\varphi + X_1 \cos\varphi \\ V = F_S^0 \cos\varphi - X_1 \sin\varphi \\ \quad M = M^0 - X_1 y \end{cases} \tag{1}$$

Table 5 Experimental and predicted peak loads of the arches

Arch	Failure mode	Maximum load (kN)	Improvement to PC arch	Improvement to RC arch	Predicted peak load(kN)	Error
RC (Zhang *et al*. 2015)	Bending failure	106.1			97.7	-7.9%
PC	Bending failure	20.6			25	21.4%
Retrofitted PC	Shear failure at vault	170.3	726.7%	60.5%	180.6	6%
Strengthened PC	Shear failure at vault	208.3	911.2%	96.3%	213.4	2.4%

with

$$M^0 = \begin{cases} \frac{P}{2} r(1-\sin\varphi), \varphi \in \left[0, \frac{\pi}{2}\right] \\ \frac{P}{2} r(1+\sin\varphi), \varphi \in \left[-\frac{\pi}{2}, 0\right] \end{cases} \quad (2)$$

$$F_S^0 = \begin{cases} \frac{P}{2}, \varphi \in \left[0, \frac{\pi}{2}\right] \\ -\frac{P}{2}, \varphi \in \left[-\frac{\pi}{2}, 0\right] \end{cases} \quad (3)$$

and

$$X_1 = \frac{P}{\pi}\frac{r^2 A}{r^2 A + I} \quad (4)$$

where N, V and M denote the axial force, the shear force and the bending moment of the structure, respectively. r is the radius of the semi-circular arch. A is the area of the cross-section and I is the second moment of the cross-section area. As shown in Fig. 8(b), the largest moment locates at the vault. Other extreme points locate at the vicinity of shoulders with α = 32.5° and α = 147.5°, where the axial force is also the largest but the sheer force is zero. Theoretically, failure will appear at the vault firstly and the shoulders subsequently, which coincides with the experimental observations, especially for the failure mode of PC arch. For semi-circular arch structure, $\alpha = \pi/2 - \varphi$. According to preceding analysis, M/P, V/P and $M/(rP)$ can be expressed as the functions of α

$$\begin{cases} N / P = F_1(\alpha) \\ V / P = F_2(\alpha) \\ M / rP = F_3(\alpha) \end{cases} \quad (5)$$

The experiments reveal two failure modes for the arches, namely bending failure and shear failure. Eq. (5) shows that the maximum load of the arch is associated with the location of destruction and the failure mode, in other words, the maximum bending moment or shear capacity of arch cross-section are the key factors. If the shoulder of the arch is eventually ruptured or destructed by bending failure, the peak load, P_u, is given by

$$P_u = 20 M_u \quad (6)$$

and M_u is the ultimate bending moment of the arch cross-section and given by

$$M_u = \frac{bh^2 \sigma_{ct}}{6} \quad (7)$$

Where σ_{ct} is the tensile strength of the concrete, and equals to 2.5 MPa. b and h denote the width and thickness of the arch's cross-section. Therefore, the peak load of the PC arch predicted by Eqs. (6) and (7) is 25 kN, a little higher than the testing result.

In terms of the CFRP retrofitted PC arch, the overall performance and the load carrying capacity had been greatly improved because of the wrapped hooped CFRP sheets. The failure mode of the CFRP retrofitted PC arch was induced by the shear failure near the vault, so the peak load is determined by

$$P_u = 2V_u \quad (8)$$

with

$$V_u = bh(\alpha_1 \sigma_{cu} + \alpha_2 \eta \sigma_{fu} \rho_{fv}) \quad (9)$$

and

$$\alpha_1 = \frac{0.2}{\lambda + 1.5} \quad (10)$$

where $\lambda = r / h$ is the shear span ratio with a value no greater than 3 in here, and the value of α_2 is 1.25 (Che 1988), ρ_{fv} represents the reinforcement ratio of hooped CFRP sheets. Shear resistance of hooped CFRP sheets depends on the reinforcement ratio ρ_{fv}, tensile strength σ_{fv} and utilizing efficiency η of CFRP sheets (Chen and Teng

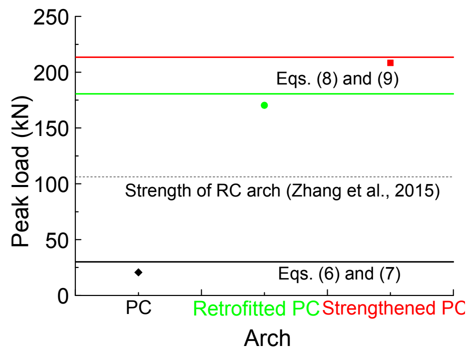

Fig. 9 Load carrying capacity of the arches.

2003, Chen *et al*. 2012), η is the ratio of CFRP stress or strain at collapse to its tensile strength or ultimate strain. Taking into account of the shear failure occurred near the vault of the CFRP retrofitted PC arch, the maximum strain of S2 is used to calculate the utilizing efficiency of CFRP sheets, inducing η = 0.368. So the peak load of the CFRP retrofitted PC arch predicted by Eq. (8) is 180.6 kN. As for the CFRP strengthened arch, η = 0.485, and the calculated peak load is 213.4 kN.

Both the experimental and predicted peak loads of the three arches are listed in Table 5. As for the CFRP retrofitted PC arch, the prediction is a little higher. As for the CFRP strengthened PC arch, the prediction is almost close to the experimental value, as shown in Fig. 9. According to the investigation, the simplified theoretical model is appropriate to analyze the simply supported composite arch structure loaded by a concentrated load on the vault.

5. Conclusions

In this research, a broken PC arch was repaired and strengthened by CFRP sheets, and its structural performance under static compression experiments was tested. A simplified theoretical model was presented to estimate the peak load of static loaded composite arches. According to the research, it is concluded that:

- The CFRP bonding/wrapping technique is an efficient method to repair and strengthen concrete arch structure, and steel reinforcements in RC arch can be replaced by bonded CFRP sheets.
- Using continuously wrapping scheme, shear failure controls the CFRP reinforced arch and leads to high rigidity and high peak load.
- With the damage location changed from the original broken location, the excellent structural performance of CFRP bonding/wrapping technique is testified, and this retrofitting method must be useful to masonry arches.
- The predicted results calculated from the simplified analyzing model are in good agreement with the experimental results, which verifies the validity of the model.

Acknowledgments

Supports from National Natural Science Foundation of China (51478465, 51508567,51308544 and 11372095), the Natural Science Foundations of Jiangsu Province (BK20150713, BK2011741 and BK20151448), State Key Laboratory of Constructional Machinery (SKLCM2016-2), State Key Laboratory of Mechanics and Control of Mechanical Structures (MCMS-0215G01) and National Technology Support Program (2014BAB15B01-02) are gratefully acknowledged.

References

Bansal, P.P., Sharma, R. and Mehta, A. (2016), "Retrofitting of RC girders using pre-stressed CFRP sheets", *Steel Compos. Struct., Int. J.*, **20**(4), 833-849.

Che, H.Y. (1988), *Concrete Structures*, (Second edition), China Architecture & Building Press, Beijing, China.

Chen, J.F. (2002), "Load-bearing capacity of masonry arch bridges reinforced with fibre reinforced polymer composites", *Adv. Struct. Eng.*, **5**(1), 37-44.

Chen, J.F. and Teng, J.G. (2003), "Shear capacity of FRP-strengthened RC beams: FRP debonding", *Constr. Build. Mater.*, **17**(1), 27-41.

Chen, B.L. and Wang, L.G. (2015), "Experimental study on flexural behavior of splicing concrete-filled GFRP tubular composite members connected with steel bars", *Steel Compos. Struct., Int. J.*, **18**(5), 1129-1144.

Chen, G.M., Teng, J.G. and Chen, J.F. (2012), "Process of debonding in RC beams shear-strengthenedwith FRP U-strips or side strips", *Int. J. Solids Struct.*, **49**(10), 1266-1282.

Chen, H.L., Zhou, J.N., Fan, H.L., Jin, F.N., Xu, Y., Qiu, Y.Y., Wang, P. and Xie, W. (2014), "Dynamic responses of buried arch structure subjected to subsurface localized impulsive loading: experimental study", *Int. J. Impact Eng.*, **65**, 89-101.

Chen, H.L., Xie, W., Jiang, M.R., Wang, P., Zhou, J.N., Fan, H.L., Zhen, Q. and Jin, F.N. (2015), "Blast-loaded behaviors of severely cracked buried arch repaired by anchored CFRP strips", *Compos. Struct.*, **122**, 92-103.

Dagher, H.J., Bannon, D.J., Davids, W.G., Lopez-Anido, R.A., Nagy, E. and Goslin, K. (2012), "Bending behavior of concrete-filled tubular FRP arches for bridge structures", *Constr. Build. Mater.*, **37**, 432-439.

D'Ambrisi, A., Focacci, F., Luciano, R., Luciano, R., Alecci, V. and Stefano, M.D. (2015), "Carbon-FRCM materials for structural upgrade of masonry arch road bridges", *Compos. Part B-Eng.*, **75**, 355-366.

Hamed, E., Chang, Z.T. and Rabinovitch, O. (2014), "Strengthening of reinforced concrete arches with externally bonded composite materials: testing and analysis", *J. Compos. Constr.*, **19**(1), 1-15.

Lu, Y.Y., Li, N., Li, S. and Ou, T.Y. (2015), "Slender RC columns strengthened with combined CFRP and steel jacket under axial load", *Steel Compos. Struct., Int. J.*, **19**(5), 1077-1094.

Su, L., Li, X. and Wang, Y. (2016), "Experimental study and modelling of CFRP-confined damaged and undamaged square RC columns under cyclic loading", *Steel Compos. Struct., Int. J.*, **21**(2), 411-427.

Sun, G.J. (2013), "The study on performance of concrete composite arch reinforced with CFRP", Dissertation; Chongqing Jiaotong University, Chongqing, China.

Wang, X. (2013), "Experimental study on strengthening concrete arch with carbon fiber reinforced polymer", Dissertation; Chongqing Jiaotong University, Chongqing, China.

Xie, W., Jiang, M.R., Chen, H.L., Zhou, J.N., Xu, Y., Wang, P., Fan, H.L. and Jin, F.N. (2014), "Experimental behaviors of CFRP cloth strengthened buried arch structure subjected to subsurface localized explosion", *Compos. Struct.*, **116**, 562-570.

Zhang, X., Wang, P., Jiang, M.R., Fan, H.L., Zhou, J.N., Li, W.X., Dong, L., Chen, H.L. and Jin, F.N. (2015), "CFRP strengthening reinforced concrete arches: Strengthening methods and experimental studies", *Compos. Struct.*, **131**, 852-867.

BU